HHS Public Access

Author manuscript

Oncogene. Author manuscript; available in PMC 2017 November 22.

Published in final edited form as:

Oncogene. 2017 September 21; 36(38): 5421–5431. doi:10.1038/onc.2017.143.

Targeting Group I p21-Activated Kinases to Control Malignant Peripheral Nerve Sheath Tumor Growth and Metastasis

Galina Semenova[1,5], **Dina S. Stepanova**[2,5], **Cara Dubyk**[3], **Elizabeth Handorf**[4], **Sergey M. Deyev**[1,6], **Alexander J. Lazar**[7], and **Jonathan Chernoff**[5,8]

[1]Shemyakin–Ovchinnikov Institute of Bioorganic Chemistry, Russian Academy of Sciences, Moscow, Russia

[2]Russian National Research Medical University, Moscow, Russia

[3]Biosample Repository, Fox Chase Cancer Center, Philadelphia, Pennsylvania

[4]Biostatistics and Bioinformatics, Fox Chase Cancer Center, Philadelphia, Pennsylvania

[5]Cancer Biology Program, Fox Chase Cancer Center, Philadelphia, PA

[6]National Research Tomsk Polytechnic University, Tomsk, Russia

[7]The University of Texas MD Anderson Cancer Center, Houston, TX

Abstract

Malignant peripheral nerve sheath tumors (MPNSTs) are devastating sarcomas for which no effective medical therapies are available. Over 50% of MPSNTs are associated with mutations in *NF1* tumor suppressor gene, resulting in activation of Ras and its effectors, including the Raf/Mek/Erk and PI3K/Akt/mTORC1 signaling cascades, and also the WNT/β-catenin pathway. As Group I p21-activated kinases (Group I Paks, PAK1/2/3) have been shown to modulate Ras-driven oncogenesis, we asked if these enzymes might regulate signaling in MPNSTs. In this study we found a strong positive correlation between the activity of PAK1/2/3 and the stage of human MPNSTs. We determined that reducing Group I Pak activity diminished MPNST cell proliferation and motility, and that these effects were not accompanied by significant blockade of the Raf/Mek/Erk pathway, but rather by reductions in Akt and β-catenin activity. Using the small molecule PAK1/2/3 inhibitor Frax1036 and the MEK1/2 inhibitor PD0325901, we showed that the combination of these two agents synergistically inhibited MPNST cell growth *in vitro* and dramatically decreased local and metastatic MPNST growth in animal models. Taken together, these data provide new insights into MPNST signaling deregulation and suggest that co-targeting of PAK1/2/3 and MEK1/2 may be effective in the treatment of patients with MPNSTs.

[8]Correspondance to: Jonathan Chernoff, Cancer Biology Program, Fox Chase Cancer Center, 333 Cottman Ave W451, Philadelphia, PA 19111, 215 728 5319, 215 728 3616 (fax), Jonathan.Chernoff@fccc.edu.

Disclosure of Potential Conflicts of Interest

No potential conflicts of interest were disclosed.

Supplementary Information accompanies thepaper on the Oncogene website (http://www.nature.com/onc).

Keywords

p21-activated kinases; malignant peripheral nerve sheath tumors; metastasis; signal transduction; small-molecule kinase inhibitors

Introduction

Malignant peripheral nerve sheath tumors (MPNSTs) are soft tissue sarcomas that originate from cells of neural crest lineage (1). Approximately half of MPNSTs develop in patients with neurofibromatosis type I (NF1), a hereditary cancer predisposition syndrome caused by inactivation of the *NF1* gene (2, 3). MPNSTs exhibit aggressive growth and a high rate of local and systemic recurrence and serve as major source of morbidity for NF1 patients (4, 5). MPNSTs have limited sensitivity to radio- and chemotherapy, while surgical resection is often hindered by the high degree of invasiveness of the tumors (3, 6).

The past decade has brought increasing efforts to identify specific diagnostic and prognostic markers associated with MPNSTs as well as relevant anticancer targets. While biallelic loss of the *NF1* gene in Schwann cells, resulting in activation of Ras signaling, is the molecular cause of the benign lesions seen in NF1 patients, secondary genetic alterations must occur for these tumors to transform into MPNSTs (1, 7), implying that additional signaling pathways contribute to MPNST pathobiology. Several studies have suggested that Mek/Erk and Akt/mTORC1 signaling are critical for MPNST tumor growth (8–11), and recent investigations have also revealed that the WNT/β-catenin pathway is activated in MPNSTs and might represent a promising therapeutic target for these conditions (12–14).

Signaling through all three of these pathways - Mek/Erk, Akt/mTORC1, and Wnt/β-catenin – can be modulated by Group I p21-activated kinases (Group I Paks, PAK1/2/3), important effectors of Rho family small GTPases RAC1 and CDC42 (15, 16). Group I Paks have been suggested to play pivotal role in the growth and dissemination of several cancers; furthermore, Pak inhibition has been shown to decrease the tumorigenic potential of different human cancer cells *in vitro* and in animal models (16, 17).

Almost twenty years ago, expression of a dominant-negative form of PAK1 was shown to reduce the anchorage-independent and xenograft growth of the NF1-mutant MPNST cell line ST8814 (18), but more physiologic approaches using genetic and pharmacologic tools are lacking. As Group I Paks regulate signaling nodes important for MPNST cell survival, proliferation and migration in several cell types (16), we speculated that PAK1/2/3 signaling may play a role in MPNST growth and metastasis. While genetic alterations of *PAK* genes in MPNSTs have not been reported, amplification of *RAC1* and several Rho-GTPase pathway genes has been described in this setting (19). RAC1 activity has been shown to be elevated in *NF1* deficient cells, contributing to increased cell proliferation and motility (20, 21).

Here, we show that PAK1/2/3 activity is significantly elevated in human MPNSTs and MPNST-derived cell lines. Importantly, this abnormal activation is most markedly noted in metastatic tumors. Exposure of MPNST cell lines to specific small-molecule and peptide

inhibitors of Group I Paks was associated with decreased motility and cell proliferation. Pak inhibition reduced β-catenin and Akt signaling in most MPSNT cells, but interestingly, did not consistently reduce activation of the Mek/Erk cascade. Dual inhibition of PAK1/2/3 and MEK1/2 resulted in synergistic inhibition of MPNST cell growth *in vitro* and markedly reduced MPNST tumor growth in xenograft and experimental metastasis models of MPNST. These data suggest that Group I Pak inhibitors might be useful for treatment of advanced MPNSTs as single agents or in combination with inhibitors of the Mek/Erk cascade.

Results

Activation of PAK1/2/3 Signaling in Human MPNSTs

To investigate the potential contribution of RAC1/Pak signaling to MPNST pathogenesis we assessed the activity of Group I Paks in a cohort of human samples. Phosphorylation of PAK1/2/3 at the Ser144/Ser141/Ser139 sites was used as readout for PAK1/2/3 activity (22). A clinically-annotated tissue microarray (TMA), containing sporadic and NF1-associated MPNST, as well as neurofibroma and normal peripheral nerve samples (Table S1), was stained for phospho-PAK1/2/3 (Fig. 1A).

We found no significant difference between Pak phosphorylation in benign tumors (neurofibromas) and normal nerve tissues; however, phospho-PAK1/2/3 immunoreactivity was markedly enhanced in MPNST specimens (Fig. 1B), in line with kinase activity of Mek and Akt (as indicated by levels of assessed phospho-proteins), as well as transcriptional activity of β-catenin (as indicated by β-catenin nuclear localization) (Supplementary Fig. S1). Furthermore, metastatic MPNSTs displayed significantly higher phospho-PAK1/2/3 levels compared to primary MPNSTs (Fig. 1B), indicating that activation of PAK1/2/3 signaling is associated with advanced peripheral nerve sheath tumor stage. No association of PAK1/2/3 activity with NF1 status of the patients was detected for either benign or malignant tumors.

We next asked if Pak, Mek and Akt activity are correlated in neurofibromas and MPNSTs. As expected, we found high association of phospho-MEK1/2 (Ser217/Ser221) and phospho-AKT (Ser473) in TMA specimens ($\rho = 0.541$, $p < 001$) (Fig. 1C). Significant associations were also identified between phospho-PAK1/2/3 and phospho-MEK1/2 levels ($\rho = 0.426$, $p < 001$), but not phospho-AKT ($\rho = 0.16$, $p = 0.298$), suggesting that Pak phosphorylation correlates with increased proliferative potential rather than survival in MPNSTs.

We further evaluated the potential function of Group I Paks by assessing RAC1, PAK1/2/3, and phospho-PAK1/2/3 protein levels in a panel of 8 human MPNST cell lines. Primary human Schwann cells (SC) lysate was used as a control for Western blot (WB) analysis. Most MPNST cell lines show altered protein levels and/or activity of PAK1/2/3 compared to normal SCs (Fig. 1D). Cell line ST8814, which was reported to have copy number gain and overexpression of *RAC1* (19), exhibited elevated levels of RAC1 protein (Supplementary Fig. S2), as well as increased levels of phospho-PAK1/2/3.

For further *in vitro* studies we picked three human MPNST cell lines with different characteristics: S462TY, an NF1-associated MPNST cell line displaying high phospho-

protein levels of PAK1/2/3; STS26T, a sporadic MPNST cell line exhibiting levels of RAC1 and phospho-PAK1/2/3 comparable to normal SC; and ST8814, NF1-associated MPNST cell line showing elevated levels of RAC1 protein and a moderate increase in PAK1/2/3 activity.

Effects of PAK1/2/3 Inhibition on Proliferation and Motility of MPNST Cells

To assess the functional role of Pak activation in MPNST cells we used two specific PAK1/2/3 inhibitors of distinct classes - GST-PID, a polypeptide inhibitor of PAK1/2/3 (23) and Frax1036, a small-molecule ATP-competitive inhibitor of PAK1/2/3 - as well as siRNA. Control immortalized human Schwann cells (iHSC) (24), and the MPNST cell lines S462TY, STS26T, and ST8814 cells were infected with recombinant retrovirus encoding GST-PID. We found that GST-PID expression nearly completely inhibited proliferation of S462TY cells, which expressed very high phospho-PAK1/2/3, and substantially suppressed proliferation of ST8814 cells, while having an insignificant effect on STS26T cells, which expressed the lowest levels of phospho-PAK1/2/3 (Fig. 2A).

For pharmaceutical Pak inhibition, MPNST cells were exposed to Frax1036. Sensitivity to the inhibitor also reflected expression/activity levels of PAK1/2/3 (S462TY>ST8814>STS26T) (Fig. 2B). Other MPNST cell lines tested (90–8, ST88–3, sNF02.2, sNF96.2 and sNF94.3) showed moderate sensitivity to Frax1036; however, the effect on cell growth similarly correlated with phospho-PAK1/2/3 levels (Supplementary Fig. S3). These observations suggest that phospho-PAK1/2/3 may be used as a potential biomarker that could define therapeutic response to Pak inhibitors.

In addition to inhibition of Pak using small molecules, we assessed the effect of knockdown of Group I Paks on MPNST proliferation. iHSC, ST8814, STS6T, and S462TY cells were transfected with siRNAs against PAK1, PAK2, and PAK3. Knockdown of Paks had little effect in iHSC cells and STS26T cells, but inhibited proliferation of ST8814 and S462Y cells (Supplementary Fig 4A).

To determine if Paks play a role in MPNST dissemination, *in vitro* functional experiments were performed to evaluate the effects of PAK1/2/3 loss-of-function on invasion. We observed a significant reduction in the invasive potential of cells expressing GST-PID (Fig. 2C, Supplementary Fig. S6). Treatment with Frax1036, or transfection with siRNAs against PAK1/2/3, elicited a similar reduction in invasive potential (Supplementary Figs. S4B and S6).

Molecular mechanisms underlying effects of PAK1/2/3 inhibition *in vitro*

To assess the mechanisms by which PAK1/2/3 contributes to MPNST cellular proliferation and motility, we analyzed key signaling pathways in iHSC, ST8814, STS26T and S462TY cells using three independent approaches: infection with a GST-PID retrovirus, exposure to Frax1036 for 24 h, or transfection of anti-Pak siRNAs. In all four cell lines, expression of GST-PID or treatment with Frax1036 effectively reduced Pak activity, as assessed by phospho-PAK1/2/3 immunoblot (Fig. 3).

The Raf/Mek/Erk cascade plays a central role in MPNST biology (9), and Group I Paks regulate Erk activity in some cell types by phosphorylating c-RAF at S338 and MEK1 at S298 (16, 25, 26). As expected, either expression of GST-PID, or treatment with Frax1036, strongly suppressed PAK1/2/3 auto-phosphorylation and MEK1 S298 phosphorylation (Fig. 3). Surprisingly, MEK1/2 S217/S221 phosphorylation levels, known to report MEK1/2 kinase activity, were not significantly reduced, despite the loss of MEK1 S298 phosphorylation (Fig. 3). The lack of effect of Pak inhibitors on Mek activity was corroborated by phospho-Erk blotting, which showed little effect of the GST-PID or Frax1036 on Erk activation in these four cell lines. Similar results were obtained in iHSC and MPNST cells in which PAK1/2/3 was knocked down by siRNA (Supplementary Fig. S6. Thus, unlike many other cell types, in MPNST cells MEK1 S298 phosphorylation is uncoupled from Mek activity, and Group I Paks are dispensable for Erk activation.

Group I Paks can also affect Akt activation, either via a scaffolding interaction with PDK1 or by direct phosphorylation (16). We found that treatment with PAK1/2/3 inhibitors or siRNA reduced phosphorylation effect on Akt (Fig. 3) and mTOR (Supplementary Figs. S6 and S7) in two of the three MPNST cell lines tested, in particular in ST8814 cells.

The Wnt/β-catenin pathway has also been implicated in MPNST maintenance (12, 14), and, in some cells, is activated by Pak signaling (16, 27, 28). We examined the effect of Pak inhibition on the Wnt/β-catenin pathway activity. ST8814, STS26T and S462TY MPNST cell lines expressing GST-PID or treated with Frax1036 showed decreases in active (non-phospho-S33/37/T41) β-catenin (Fig. 3). These data suggest that PAK1/2/3 may promote MPNST growth, invasion and metastasis via β-catenin stabilization.

As β-catenin signaling activates expression of genes involved in cell motility and invasion transition (29, 30), we examined profiles of E- and N-cadherin expression in cells treated with Pak inhibitors. Loss of E-cadherin expression and the upregulation of N-cadherin expression generally correlate with increased tumor cell motility and invasion (31). Mature myelinating SCs express E-cadherin, a key component of adherens junctions, while N-cadherin is a marker of motile SC precursors (32). Immunoblot analysis of MPNST cell lysates revealed that N-cadherin was present in ST8814, STS26T and S462TY cells, and that treatment with Pak inhibitors significantly reduced N-cadherin levels (Fig. 3 and Supplementary Fig. S7). ST8814 cells expressing GST-PID or exposed to Frax1036 showed an N-cadherin-to-E-cadherin switch, typical for SC differentiation, suggesting that Group I Paks may promote MPNST invasion and metastasis in part by regulating cadherin expression.

Importantly, cells with higher phospho-PAK 1/2/3 (ST8814 and, especially, S462TY) were more sensitive to PAK1/2/3 inhibition and showed more significant effect on Akt, β-catenin signaling and cadherin switch when PAK1/2/3 is inhibited. STS26T (sporadic MPNST cell line with low pPAK and poor sensitivity to Pak inhibitors), as well as control iHSC, showed little or no change in indicated pathways upon PAK1/2/3 inhibition.

Synergistic effects of PAK1/2/3 and MEK1/2 dual inhibition *in vitro*

Considering that Pak ablation alone was not sufficient to suppress Erk phosphorylation (Fig. 3), we hypothesized that addition of a Mek inhibitor might increase the antiproliferative effect of Frax1036. We found that the MEK1/2 inhibitor PD-0325901 (PD-901) (34) eliminated Erk phosphorylation (Fig. 4A) and synergized with Frax1036 in limiting proliferation in ST8814, STS26T and S462TY MPNST cells (Fig. 4B). MPNST cell lines treated with varying dilutions of Frax1036 and PD-901 at their respective IC_{50}s resulted in Chou-Talalay combination indices (CI) below 1.0, suggesting that combined Pak and Mek inhibition synergistically supresses MPNST cellular growth. Likewise, the growth of control iHSC was synergistically inhibited by a combination of Frax1036 and PD-901; however, higher doses of both inhibitors were required to achieve this effect.

Effects of PAK1/2/3 and MEK1/2 pharmaceutical inhibition on MPNST xenograft tumor growth

To determine whether our *in vitro* observations suggest therapies applicable *in vivo*, we investigated the antitumor efficacy of the PAK1/2/3 inhibitor Frax1036 as monotherapy and in combination with the MEK1/2 inhibitor PD-901 in subcutaneous xenografts of S462TY and STS26T human MPNSTs. Therapy was initiated after establishment of tumor (average 100 mm^3). Tumor-bearing mice were treated with vehicle, Frax1036 (30 mg/kg/day), PD-901 (10 mg/kg/day) or the combination of Frax1036 (30 mg/kg/day) and PD-901 (5 mg/kg/day) for a period of 4 weeks (Fig. 5).

Treatment with Frax1036 monotherapy slightly attenuated the growth of STS26T xenografts (~1302.09 mm^3 versus ~1915.5 mm^3 in control group at study termination, $p = 0.051$), while tumors in mice receiving PD-901 alone were significantly smaller (~288 mm^3, $p = 0.002$). The combination of Frax1036 and PD-901 induced marked tumor regression (~25.7 mm^3, $p = 0.002$) (Fig. 5A). Mice were sacrificed at day 28 after treatment initiation and xenograft tumor tissues were collected. Histological analysis revealed a significant decrease in the number of phospho-histone 3 (pHH3)-positive cells in tumors exposed to the combination of Frax1036 and PD-901. Although tumors regressed in mice treated with the combination of inhibitors, apoptosis was not observed, as indicated by cleaved caspase 3 (CC3) staining (Fig. 5B), suggesting that by the end of the prolonged exposure to the inhibitors, cytostatic effects prevailed.

In S462TY xenograft experiments, only mice treated with a combination of Frax1036 and PD-901 survived until at least experimental day 28 (~700.4 mm^3 at study termination). The control group required sacrifice at day 13 (~2241.1 mm3), PD-901-treated mice at day 19 (~2231.1 mm^3) and Frax1036 treated mice at day 22 (~2232.4 mm3) (Fig. 5A). IHC staining confirmed reduced levels of pHH3 as well as elevated levels of CC3 present in tumor tissues isolated from combinatorial treatment group (Fig. 5B).

Therapy was well tolerated in all experimental groups with no apparent toxicities (Supplementary Fig. S8). Inhibition of PAK1/2/3 and ERK1/2 activity by Frax1036 and PD-901 was confirmed by WB analysis of tumor protein lysates. Consistent with the *in vitro*

data, treatment with Frax1036 in both STS26T and S462TY xenograft models did not alter ERK1/2 phosphorylation levels (Supplementary Fig. S9).

Effects of Pak1/2/3 and MEK1/2 pharmaceutical inhibition growth of experimental MPNST lung metastases

Given that PAK1/2/3 ablation regulates molecular mechanisms driving MPNST invasive growth and has a suppressive effect on MPNST cell motility *in vitro*, we considered that Group I Paks might represent an attractive target for controlling MPNST metastasis. As there is no established *in vivo* model for spontaneous MPNST metastasis, we used a previously described experimental metastasis model, in which tail vein injection of tumor cells leads to the formation of microcolonies in the lung (35). Of the MPNST cells available to us, we selected STS26T, as these are, to our knowledge, the only available MPNST cells known to cause lung tumors after tail vein injection (35).

Luciferase-labeled STS26T cells (STS26T-Luc) were injected into the tail vein of SCID immunodeficient mice. To evaluate whether Frax1036 alone or combined with PD-901 can prevent MPNST cells from forming colonies in the lungs, we started exposure to the inhibitors on the day of injection. The Mek inhibitor PD-901 was used at the lower dose of 5 mg/kg/d to reduce its effects on cell proliferation. Mice were allocated to four groups and treated with placebo, Frax1036 (30 mg/kg/day), PD-901 (5 mg/kg/day) or the combination of Frax1036 (30 mg/kg/day) and PD-901 (5mg/kg/day) for a period of 3 weeks, and monitored by bioluminescent imaging (BLI).

BLI imaging indicated inhibition of tumor growth rate in mice treated with Frax1036 (~7677.143 p/s/cm^2/sr) or PD-901 (~11025.71 p/s/cm^2/sr) compared to untreated mice (~18112.86 p/s/cm^2/sr) (Fig. 6A). Significantly, in mice exposed to combination of Frax1036 and PD-901, BLI signals remained comparable to background throughout the experiment (2760 p/s/cm^2/sr *versus* 2084.64 p/s/cm^2/sr background) (Fig. 6A). Endpoint assessments confirmed these observations, showing significant difference in average lung weight between control (~329.7 mg/~1.75% body weight) and Frax1036 (~195.3 mg/~0.97% body weight) or PD-901-treated groups (~196.4 mg/~0.92% body weight). In contrast, the lung weight was normal in mice treated with both Frax1036 and PD-901 (~149.4 mg/~0.75% body weight) (Fig. 6C).

Large tumor deposits were observed in 6 out of 7 control mice as indicated by H&E staining of pathological lung specimens collected (Fig. 6B). Metastases in abdominal lymph nodes were found in 3 control mice, metastases in ovaries were found in 1 control mouse (data not shown). Smaller lung lesions were observed in Frax1036 and PD-901-treated groups, while mice under combinatorial treatment had no histologically detected tumors (Fig. 6B).

Discussion

The invasive and metastatic nature of MPNSTs presents a major therapeutic challenge. While several studies have focused on the molecular mechanisms of MPNST initiation and growth, the mechanisms of MPNST dissemination are largely unexplored. Based on a number of prior studies showing that Pak regulates Erk, Akt, and β-catenin activity (16) –

three signaling nodes important in MPNSTs (9, 10, 12, 14) - we here investigated the role of Group I Paks in MPNST pathobiology, with the idea that Pak isoforms might represent promising targets for growth and metastasis of these tumors.

We found that PAK1/2/3 phospho-protein levels are elevated in MPNSTs compared to normal nerves. This was not observed in NF1–associated neurofibromas, suggesting that *NF1* loss alone is not sufficient for up-regulation of PAK1/2/3, and that additional Ras-independent signals must contribute to Pak activation in MPNSTs. Similarly, no difference in Pak activity was found between sporadic and NF1-asociated MPNSTs. At the same time, phospho-PAK1/2/3 staining was significantly stronger in MPNST metastases compared to primary MPNSTs, indicating that Group I Pak signaling is important for tumor formation and growth at distant organs.

To our knowledge, only one previous study has examined the role of Paks in MPNSTs (18). In that work, the authors found that expression of a dominant-negative form of PAK1 inhibited MPNST growth in the ST8814 cell line, presumably through down-regulation of Erk (9). Here we used a peptide inhibitor of Group I Paks GST-PID, as well as a highly selective small molecule PAK1/2/3 inhibitor Frax1036, to show that Pak down-regulation impeded the growth and motility of three distinct MPSNT cell lines: ST8814, STS26T and S462TY. Interestingly, these effects were not associated with consistent loss of Erk activity, despite effective inhibition of PAK1/2/3 and suppressive effects on β-catenin activation by Frax1036, GST-PID, and PAK1/2/3 knockdown. PAK1/2/3 inhibition effectively suppressed the invasiveness of MPNST cells, with more moderate effects on the proliferation of ST8814 and STS26T cells. Of the cell lines tested, S462TY cells, which exhibited strikingly high levels of PAK1 and phospho-PAK1/2/3, were exquisitely sensitive to Pak inhibition. This finding is in line with recent studies on Pak function in breast and ovarian cancer cells, in which overexpression of PAK1 is associated with “addiction” to this kinase (35, 36). Similarly, the effect of Frax1036 on tumor growth was most striking for S462TY xenografts and more modest for STS26T tumors. However, even in the sensitive S462TY cell line, Pak inhibition did not reduce Erk activation, suggesting that Pak is not strongly linked to the Mek/Erk pathway in MPNST cells.

Given the importance of Mek/Erk signaling in MPNSTs, we investigated whether Frax1036 might cooperate with the Mek inhibitor PD0325901 (PD-901). PD-901 was previously tested in several preclinical studies and has shown moderate efficacy as a single agent in MPNST models (9, 37). In clinical trials, PD-901 had adverse effects and did not meet its primary efficacy endpoint (38–40), suggesting the need to identify drug combinations that effectively suppress tumor growth while minimizing toxicity. By combining the Pak inhibitor Frax1036 with PD-901, we achieved synergistic inhibition of cell growth in MPNST cell lines and more effectively inhibited xenograft tumor growth than by targeting either pathway alone. The combination of Frax1036 with PD-901 was effective with a reduced dose of PD-901, and this combination was well-tolerated. PAK1/2/3 inhibition caused a decrease in the invasive potential of MPNST cells, associated with a reduction of β-catenin activity and N-cadherin expression. The ST8814 cell line also showed an increase of E-cadherin expression in response to Frax1036 or GST-PID. The consequences of such alterations in cell adhesion molecules expression in MPNSTs require further investigation.

Loss of the mesenchymal marker N-cadherin and gain of E-cadherin might strengthen intracellular contacts, preventing MPNST cells breakage from the tumor mass and migration into blood vessels. On the other hand, obtaining an epithelial phenotype might give an advantage for metastases in distant organs. To rule out this scenario we have used an experimental MPNST lung metastasis model (Fig. 6.) and showed that, in fact, treatment with Frax1036 inhibits both grafting MPNST cells in the lungs and growth of metastatic tumors, while combination of Frax1036 and PD-901 practically eliminated formation and growth of metastases. These results suggest that PAK1/2/3 is a reasonable target for MPNSTs, especially when combined with a Mek inhibitor, which has a strong anti-proliferative effect. As highly specific small molecule inhibitors of Group I Paks have been developed (41), including an isoform specific inhibitor of PAK1 (42), it is reasonable to consider that such inhibitors, alone or in combination with a Mek inhibitor, will be useful in the treatment of MPNSTs

Materials and Methods

Cell Lines

MPNST cell lines sNF96.2, sNF02.2 and sNF94.3 were obtained from the American Type Culture Collection, STS26T and S462TY were generously provided by Dr. Timothy Cripe (Nationwide Children's Hospital, OH), ST8814, ST88–3 and 90–8 were generously provided by Dr. Nancy Ratner (Cincinnati Children's Hospital, OH). Immortalized human Schwann cells (iHSC)were were generously provided by Dr. Ahmet Hoke (Johns Hopkins University, MD). MPNST cells were maintained in DMEM supplemented with 10% FBS and penicillin/streptomycin and cultured on tissue culture-treated plates at 37°C in 5% CO_2. iHSC were maintained in 10%FBS/DMEM supplemented with pen/strep and 2uM Forskolin (Sigma F6886). Cells were routinely tested for mycoplasma. No cell line authentication was performed.

Retroviral Transduction

For GST-PID production retroviral expression vector pBMN-GST-PID was used (23). The ΦNX packaging cells (Orbigen) were transfected using Lipofectamine-2000 reagent (Invitrogen). Viral supernatants were harvested 48 h post-transfection and filtered. MPNST cells were incubated with retroviral supernatant supplemented with 4 μg/ml polybrene for 4 h at 37 °C, and then were cultured in growth media for 48 h for viral integration. GFP-positive cells were collected by flow cytometry.

For *in vivo* imaging, STS26Tcells were transduced with a retroviral construct encoding the firefly luciferase gene (pWZL-Luc) as described above, and selected in 100 μg/mL hygromycin B.

siRNA Transfection

The cells were transfected with siRNA smartpool oligonucleotides (10 nM) targeting PAK1, PAK2 or PAK3 (Dharmacon) using RNAiMax Reagent (Invitrogen) according to the manufacturer's protocol. Non-target siRNA was used as a control.

In Vitro Cytotoxicity Assay, IC_{50}, and Combination Index (CI) Calculations

MPNST cell lines were plated in 96-well plates at 5000 cells/well in complete medium. 24 hours after plating, varied doses of inhibitors were added in triplicate. 0.1% DMSO was used as negative control. Cell viability was evaluated after 72-hour incubation with drugs using alamarBlue fluorescent assay (Life Technologies). Synergistic effects were determined by the Chou/Talalay method (45). IC_{50} and CI values were calculated using Calcusyn (Biosoft); (CI) < 1 was defined as synergism. Frax1036 and PD-901 were assumed as having independent modes of action and therefore mutually nonexclusive.

Immunoblotting

WB assay was performed using standard techniques. Primary antibodies used in this study were: p-PAK1(S144)/PAK2(S141), PAK1, PAK2, PAK3, PAK1/2/3, p-MEK1(S298), p-MEK1/2(S217/221), MEK1/2, p-ERK1/2 (T202/Y204), ERK1/2, non-phospho (Active) β-catenin, N-cadherin, β-actin from CST, E-cadherin, β-catenin from BD Biosciences, GPDH from Abcam, RAC1 from Millipore.

Invasion Assay

The assay was performed in 24-well transwell chambers (BD Biosciences) with 8-um-pore membrane. MPNST cells (10^5 STS26T cells and 5×10^5 ST8814 or S462TY cells) suspended in serum-free medium were added to the inside of the transwell insert precoated with matrigel, and the insert was then placed in a plate containing complete culture medium. After 18 h, cells on the inside were removed, cells on the underside of the insert were fixed with 4% paraformaldehyde and stained with crystal violet solution and counted under light microscope.

Animal Models

All animal procedures were performed in accordance with IACUC guides and regulations.

Female 6–7 weeks old *nu/nu* mice were injected subcutaneously with 10^6 STS26T cells or 10^7 S462TY cells in 0.1 ml 30% Matrigel (BD Biosciences)/PBS. Treatment started when the average tumor size reached 100 mm^3. Frax1036 was formulated in 20% 2-hydroxypropyl-β-cyclodextrin in 50 mM citrate buffer (pH 3.0) and administrated by oral gavage at 30 mg/kg/day. PD0325901 was prepared as a suspension in aqueous 0.5% hypromellose/0.2% Tween 80 and administrated by daily gavage at 5 or 10 mg/kg. Mice were sacrificed when tumor size reached 10% of body weight. Tumors were resected, individual portions of tumors were snap-frozen in liquid nitrogen for preparation of protein lysates, and fixed in formalin and paraffin embedded for immunohistochemical studies.

For studies of metastasis, pWZL-Luc transduced STS26T cells (10^6 cells in 0.1 ml PBS) were injected into the tail vein of 4–8 week old female SCID mice. Frax1036 (30 mg/kg/day) and/or PD0325901 (5 mg/kg/day) were administrated daily by oral gavage. Dissemination of STS26T-Luc cells was monitored weekly using bioluminescence imaging. Mice were sacrificed after three weeks of treatment. Lungs were resected, weighed, fixed and paraffin-embedded for H&E staining.

Simple randomization was used in all animal experiments. Blinding was not possible.

Bioluminescence Imaging (BLI)

For detection of growth of STS26T-Luc cells, mice were anesthetized with 3% isofluorane and given i.p. injections of RediJect D-Luciferin Ultra (Perkin Elmer) ten minutes prior to imaging using the IVIS Spectrum *in vivo* imaging system (Caliper Life Sciences) as described (46). Image analysis was performed and total flux emission (photons/second) in the region of interest was determined using the Living Image Software for the IVIS Spectrum.

Immunohistochemistry

Tisues were fixed overnight in 4**%** paraformaldehyde, dehydrated and embedded in paraffin according to standard protocols. IHC was performed with antibodies for anti-cleaved caspase-3 (CC3) and p-Histone H3 (S10) (pHH3) (Cell Signaling Technology).

A tissue microarray (TMA), containing specimens retrieved from human MPNSTs (n=207), neurofibromas (n=56) and normal nerves (n=11) surgical resections, was used to assess phospho-PAK1/2/3 levels. Tissue sections were blocked for 20 minutes and heat-induced antigen retrieval was performed in pH 6 Citrate Buffer for 20 minutes. Endogenous peroxidases were quenched with 3% hydrogen peroxide in methanol for 10 minutes. The sections were incubated overnight with phopho-PAK1/2/3 primary antibodies (Abcam) at 4°C. Anti-rabbit secondary antibodies (Dako) were incubated for 1 h at room temperature and visualized using DAB+ chromogen (Dako). Images were captured using the Vectra Automated Quantitative Pathology Imaging System and analyzed using inForm image analysis software (PerkinElmer, Caliper Life Sciences).

All human subject studies were approved by respective institutional review boards.

Statistics

p values were determined by two-tailed Student's *t*-test with Welch's correction for all *in vitro* studies. For xenograft and experimental metastasis studies, *p*-values were calculated by Mann-Whitney test. No statistical methods were used to pre-determine sample sizes. Correlations between categorical variables were performed using the $\chi 2$-test or Fisher's exact test when the number of observations obtained for analysis was small. The relationships between phospho-PAK1/2/3, phospho-MEK1/2 and phospho-AKT1/2 in TMA studies were assessed using Spearman's correlation. Linear regression was used to define significance, and potential within-subject correlation was accounted for using Generalized Estimating Equations with robust standard errors. Phospho-PAK1/2/3 H-score was log-transformed prior to analysis.

Supplementary Material

Refer to Web version on PubMed Central for supplementary material.

Acknowledgments

We thank Timothy Cripe and Nancy Ratner for providing MPNST cell lines, Ahmet Hoke for providing immortalized HSC, Maureen Murphy for providing construct pWZL-Luc, Genentech for providing Frax1036, and Erica Golemis for commentary. This work was supported by grants from the NIH (RO1 CA142928), and the Children's Tumor Foundation (2011-15-012) to Jonathan Chernoff, NIH CORE Grant P30 CA006927 and an appropriation fromthe state of Pennsylvania to the Fox Chase Cancer Center. *In vitro* studies were supported by RSF grant 14-24-00106.

References

1. Carroll SL, Ratner N. How does the Schwann cell lineage form tumors in NF1? Glia. 2008; 56:1590–1605. [PubMed: 18803326]
2. Widemann BC. Current status of sporadic and neurofibromatosis type 1-associated malignant peripheral nerve sheath tumors. Current oncology reports. 2009; 11:322–328. [PubMed: 19508838]
3. Katz D, Lazar A, Lev D. Malignant peripheral nerve sheath tumour (MPNST): the clinical implications of cellular signalling pathways. Expert reviews in molecular medicine. 2009; 11:e30. [PubMed: 19835664]
4. Tonsgard JH. Clinical manifestations and management of neurofibromatosis type 1. Seminars in pediatric neurology. 2006; 13:2–7. [PubMed: 16818170]
5. Kolberg M, Holand M, Agesen TH, Brekke HR, Liestol K, Hall KS, et al. Survival meta-analyses for >1800 malignant peripheral nerve sheath tumor patients with and without neurofibromatosis type 1. Neuro-oncology. 2013; 15:135–147. [PubMed: 23161774]
6. Packer RJ, Rosser T. Therapy for plexiform neurofibromas in children with neurofibromatosis 1: an overview. Journal of child neurology. 2002; 17:638–641. discussion 646–651. [PubMed: 12403563]
7. Carroll SL. Molecular mechanisms promoting the pathogenesis of Schwann cell neoplasms. Acta neuropathologica. 2012; 123:321–348. [PubMed: 22160322]
8. Malone CF, Fromm JA, Maertens O, DeRaedt T, Ingraham R, Cichowski K. Defining key signaling nodes and therapeutic biomarkers in NF1-mutant cancers. Cancer discovery. 2014; 4:1062–1073. [PubMed: 24913553]
9. Jessen WJ, Miller SJ, Jousma E, Wu J, Rizvi TA, Brundage ME, et al. MEK inhibition exhibits efficacy in human and mouse neurofibromatosis tumors. J Clin Invest. 2013; 123:340–347. [PubMed: 23221341]
10. Johansson G, Mahller YY, Collins MH, Kim MO, Nobukuni T, Perentesis J, et al. Effective in vivo targeting of the mammalian target of rapamycin pathway in malignant peripheral nerve sheath tumors. Molecular cancer therapeutics. 2008; 7:1237–1245. [PubMed: 18483311]
11. Endo M, Yamamoto H, Setsu N, Kohashi K, Takahashi Y, Ishii T, et al. Prognostic significance of AKT/mTOR and MAPK pathways and antitumor effect of mTOR inhibitor in NF1-related and sporadic malignant peripheral nerve sheath tumors. Clinical cancer research: an official journal of the American Association for Cancer Research. 2013; 19:450–461. [PubMed: 23209032]
12. Mo W, Chen J, Patel A, Zhang L, Chau V, Li Y, et al. CXCR4/CXCL12 mediate autocrine cell-cycle progression in NF1-associated malignant peripheral nerve sheath tumors. Cell. 2013; 152:1077–1090. [PubMed: 23434321]
13. Luscan A, Shackleford G, Masliah-Planchon J, Laurendeau I, Ortonne N, Varin J, et al. The activation of the WNT signaling pathway is a Hallmark in neurofibromatosis type 1 tumorigenesis. Clinical cancer research: an official journal of the American Association for Cancer Research. 2014; 20:358–371. [PubMed: 24218515]
14. Watson AL, Rahrmann EP, Moriarity BS, Choi K, Conboy CB, Greeley AD, et al. Canonical Wnt/beta-catenin signaling drives human schwann cell transformation, progression, and tumor maintenance. Cancer discovery. 2013; 3:674–689. [PubMed: 23535903]
15. Eswaran J, Soundararajan M, Kumar R, Knapp S. UnPAKing the class differences among p21-activated kinases. Trends in biochemical sciences. 2008; 33:394–403. [PubMed: 18639460]
16. Radu M, Semenova G, Kosoff R, Chernoff J. PAK signalling during the development and progression of cancer. Nature reviews Cancer. 2014; 14:13–25. [PubMed: 24505617]
17. Ye DZ, Field J. PAK signaling in cancer. Cellular logistics. 2012; 2:105–116. [PubMed: 23162742]

18. Tang Y, Marwaha S, Rutkowski JL, Tennekoon GI, Phillips PC, Field J. A role for Pak protein kinases in Schwann cell transformation. Proceedings of the National Academy of Sciences of the United States of America. 1998; 95:5139–5144. [PubMed: 9560242]
19. Upadhyaya M, Spurlock G, Thomas L, Thomas NS, Richards M, Mautner VF, et al. Microarray-based copy number analysis of neurofibromatosis type-1 (NF1)-associated malignant peripheral nerve sheath tumors reveals a role for Rho-GTPase pathway genes in NF1 tumorigenesis. Human mutation. 2012; 33:763–776. [PubMed: 22331697]
20. Ingram DA, Hiatt K, King AJ, Fisher L, Shivakumar R, Derstine C, et al. Hyperactivation of p21(ras) and the hematopoietic-specific Rho GTPase, Rac2, cooperate to alter the proliferation of neurofibromin-deficient mast cells in vivo and in vitro. The Journal of experimental medicine. 2001; 194:57–69. [PubMed: 11435472]
21. Dasgupta B, Li W, Perry A, Gutmann DH. Glioma formation in neurofibromatosis 1 reflects preferential activation of K-RAS in astrocytes. Cancer research. 2005; 65:236–245. [PubMed: 15665300]
22. Chong C, Tan L, Lim L, Manser E. The mechanism of PAK activation. Autophosphorylation events in both regulatory and kinase domains control activity. The Journal of biological chemistry. 2001; 276:17347–17353. [PubMed: 11278486]
23. Chow HY, Stepanova D, Koch J, Chernoff J. p21-Activated kinases are required for transformation in a cell-based model of neurofibromatosis type 2. PloS one. 2010; 5:e13791. [PubMed: 21072183]
24. Chow HY, Dong B, Duron SG, Campbell DA, Ong CC, Hoeflich KP, et al. Group I Paks as therapeutic targets in NF2-deficient meningioma. Oncotarget. 2015; 6:1981–1994. [PubMed: 25596744]
25. Deacon SW, Beeser A, Fukui JA, Rennefahrt UE, Myers C, Chernoff J, et al. An isoform-selective, small-molecule inhibitor targets the autoregulatory mechanism of p21-activated kinase. Chemistry & biology. 2008; 15:322–331. [PubMed: 18420139]
26. Slack-Davis JK, Eblen ST, Zecevic M, Boerner SA, Tarcsafalvi A, Diaz HB, et al. PAK1 phosphorylation of MEK1 regulates fibronectin-stimulated MAPK activation. The Journal of cell biology. 2003; 162:281–291. [PubMed: 12876277]
27. Beeser A, Jaffer ZM, Hofmann C, Chernoff J. Role of group A p21-activated kinases in activation of extracellular-regulated kinase by growth factors. The Journal of biological chemistry. 2005; 280:36609–36615. [PubMed: 16129686]
28. Arias-Romero LE, Villamar-Cruz O, Huang M, Hoeflich KP, Chernoff J. Pak1 kinase links ErbB2 to beta-catenin in transformation of breast epithelial cells. Cancer research. 2013; 73:3671–3682. [PubMed: 23576562]
29. He H, Huynh N, Liu KH, Malcontenti-Wilson C, Zhu J, Christophi C, et al. P-21 activated kinase 1 knockdown inhibits beta-catenin signalling and blocks colorectal cancer growth. Cancer letters. 2012; 317:65–71. [PubMed: 22100495]
30. MacDonald BT, Tamai K, He X. Wnt/beta-catenin signaling: components, mechanisms, and diseases. Developmental cell. 2009; 17:9–26. [PubMed: 19619488]
31. Barker N. The canonical Wnt/beta-catenin signalling pathway. Methods in molecular biology. 2008; 468:5–15. [PubMed: 19099242]
32. Yang J, Du X, Wang G, Sun Y, Chen K, Zhu X, et al. Mesenchymal to epithelial transition in sarcomas. European journal of cancer. 2014; 50:593–601. [PubMed: 24291235]
33. Crawford AT, Desai D, Gokina P, Basak S, Kim HA. E-cadherin expression in postnatal Schwann cells is regulated by the cAMP-dependent protein kinase a pathway. Glia. 2008; 56:1637–1647. [PubMed: 18551621]
34. Brown AP, Carlson TC, Loi CM, Graziano MJ. Pharmacodynamic and toxicokinetic evaluation of the novel MEK inhibitor, PD0325901, in the rat following oral and intravenous administration. Cancer chemotherapy and pharmacology. 2007; 59:671–679. [PubMed: 16944149]
35. Torres KE, Zhu QS, Bill K, Lopez G, Ghadimi MP, Xie X, et al. Activated MET is a molecular prognosticator and potential therapeutic target for malignant peripheral nerve sheath tumors. Clinical cancer research: an official journal of the American Association for Cancer Research. 2011; 17:3943–3955. [PubMed: 21540237]

36. Shrestha Y, Schafer EJ, Boehm JS, Thomas SR, He F, Du J, et al. PAK1 is a breast cancer oncogene that coordinately activates MAPK and MET signaling. Oncogene. 2012; 31:3397–3408. [PubMed: 22105362]

37. Prudnikova TY, Villamar-Cruz O, Rawat SJ, Cai KQ, Chernoff J. Effects of p21-activated kinase 1 inhibition on 11q13-amplified ovarian cancer cells. Oncogene. 2015

38. Watson AL, Anderson LK, Greeley AD, Keng VW, Rahrmann EP, Halfond AL, et al. Co-targeting the MAPK and PI3K/AKT/mTOR pathways in two genetically engineered mouse models of schwann cell tumors reduces tumor grade and multiplicity. Oncotarget. 2014; 5:1502–1514. [PubMed: 24681606]

39. LoRusso PM, Krishnamurthi SS, Rinehart JJ, Nabell LM, Malburg L, Chapman PB, et al. Phase I pharmacokinetic and pharmacodynamic study of the oral MAPK/ERK kinase inhibitor PD-0325901 in patients with advanced cancers. Clinical cancer research: an official journal of the American Association for Cancer Research. 2010; 16:1924–1937. [PubMed: 20215549]

40. Bain J, Plater L, Elliott M, Shpiro N, Hastie CJ, McLauchlan H, et al. The selectivity of protein kinase inhibitors: a further update. The Biochemical journal. 2007; 408:297–315. [PubMed: 17850214]

41. Haura EB, Ricart AD, Larson TG, Stella PJ, Bazhenova L, Miller VA, et al. A phase II study of PD-0325901, an oral MEK inhibitor, in previously treated patients with advanced non-small cell lung cancer. Clinical cancer research: an official journal of the American Association for Cancer Research. 2010; 16:2450–2457. [PubMed: 20332327]

42. Ndubaku CO, Crawford JJ, Drobnick J, Aliagas I, Campbell D, Dong P, et al. Design of Selective PAK1 Inhibitor G-5555: Improving Properties by Employing an Unorthodox Low-pK a Polar Moiety. ACS medicinal chemistry letters. 2015; 6:1241–1246. [PubMed: 26713112]

43. Karpov AS, Amiri P, Bellamacina C, Bellance MH, Breitenstein W, Daniel D, et al. Optimization of a Dibenzodiazepine Hit to a Potent and Selective Allosteric PAK1 Inhibitor. ACS medicinal chemistry letters. 2015; 6:776–781. [PubMed: 26191365]

44. Limame R, Wouters A, Pauwels B, Fransen E, Peeters M, Lardon F, et al. Comparative analysis of dynamic cell viability, migration and invasion assessments by novel real-time technology and classic endpoint assays. PloS one. 2012; 7:e46536. [PubMed: 23094027]

45. Chou TC, Talalay P. Quantitative analysis of dose-effect relationships: the combined effects of multiple drugs or enzyme inhibitors. Advances in enzyme regulation. 1984; 22:27–55. [PubMed: 6382953]

46. Connolly DC, Hensley HH. Xenograft and Transgenic Mouse Models of Epithelial Ovarian Cancer and Non Invasive Imaging Modalities to Monitor Ovarian Tumor Growth In situ -Applications in Evaluating Novel Therapeutic Agents. Current protocols in pharmacology/editorial board, SJ Enna. 2009; 45:14 12 11–14 12 26.

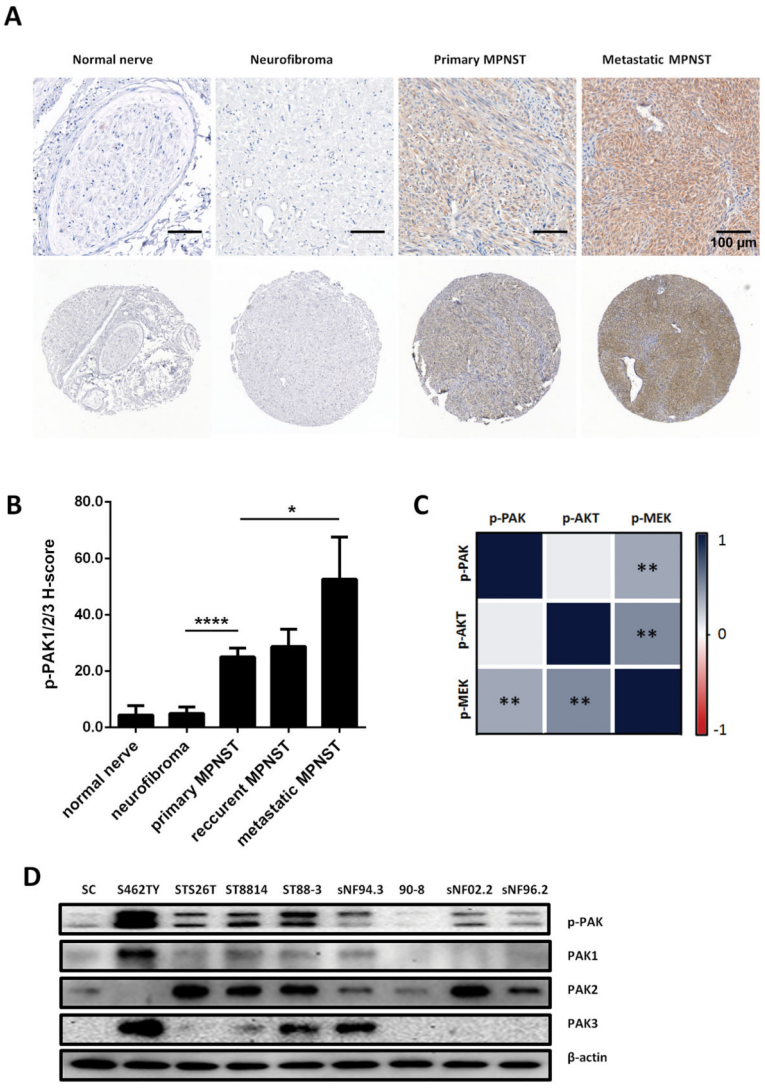

Figure 1. Phospho-PAK1/2/3 is present at high levels in human MPNST specimens and human MPNST cell lines

A, Representative photographs of MPNST tissue microarray (TMA), IHC stained for phospho-PAK1/2/3. B. Quantification of phospho-PAK1/2/3 staining intensity in MPNST TMA. C. Expression correlations between phospho-PAK1/2/3, phospho-MEK and phospho-AKT, increasing saturation of blue indicates higher correlation. D. Immunoblot analysis demonstrating Group I Pak protein and phospho-protein levels in human Schwann cells (SC) and human MPNST cell lines. Error bars represent standard error of the mean (*= $p<0.05$, **= $p<0.001$, ****= $p<0.0001$).

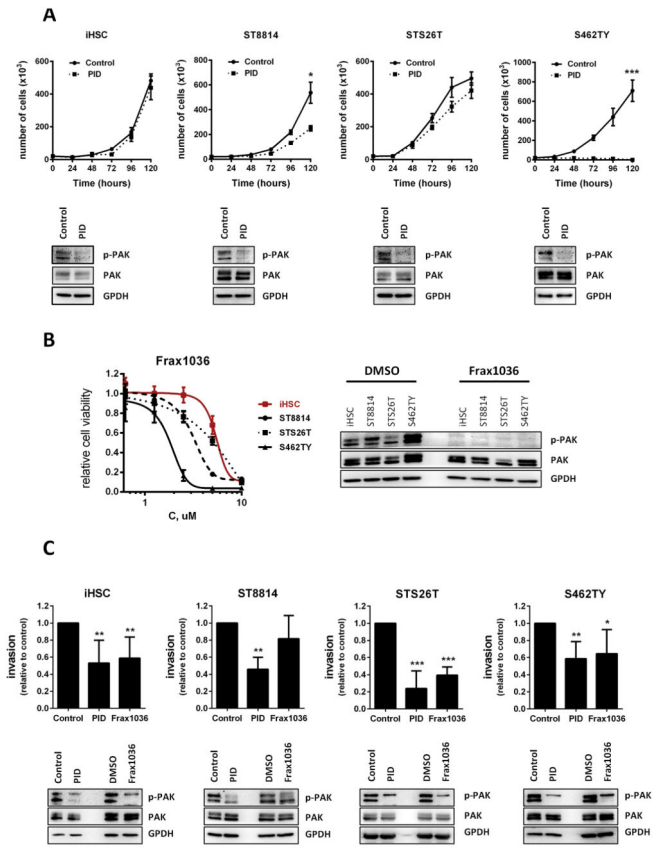

Figure 2. Group I Pak inhibitors reduce MPNST cell proliferation and invasion

A. Suppressive effect of peptide PAK1/2/3 inhibitor GST-PID on iHSC, ST8814, STS26T and S462TY cell growth. **B.** Dose response to a small molecule PAK1/2/3 inhibitor Frax1036 in iHSC and MPNST cells. **C.** Invasiveness of iHSC and MPNST cells treated PAK1/2/3 inhibitors determined by trans-matrigel invasion assay. Error bars represent standard deviation (*= p<0.05, **= p<0.01, ***= p<0.005).

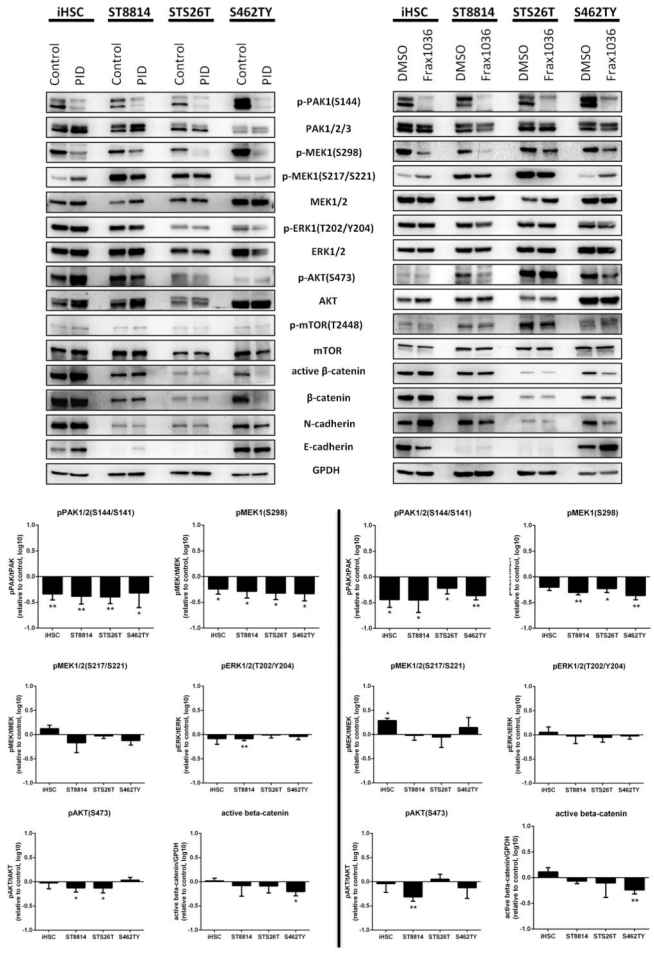

Figure 3. Inhibition of PAK1/2/3 affects MAPK, Akt, β-catenin pathways and cadherin expression

Immunoblot analysis of MAPK, AKT/mTOR and β-catenin cascades signaling and N- and E-cadherin protein levels changes in iHSC, ST8814, STS26T and S462TY cells exposed to PAK1/2/3 inhibitors GST-PID and Frax1036. WB quantification of Pak, Mek/Erk, Akt/mTOR phosphorylation changes and changes of active β-catenin levels Error bars represent standard deviation (*= $p<0.05$, **= $p<0.01$).

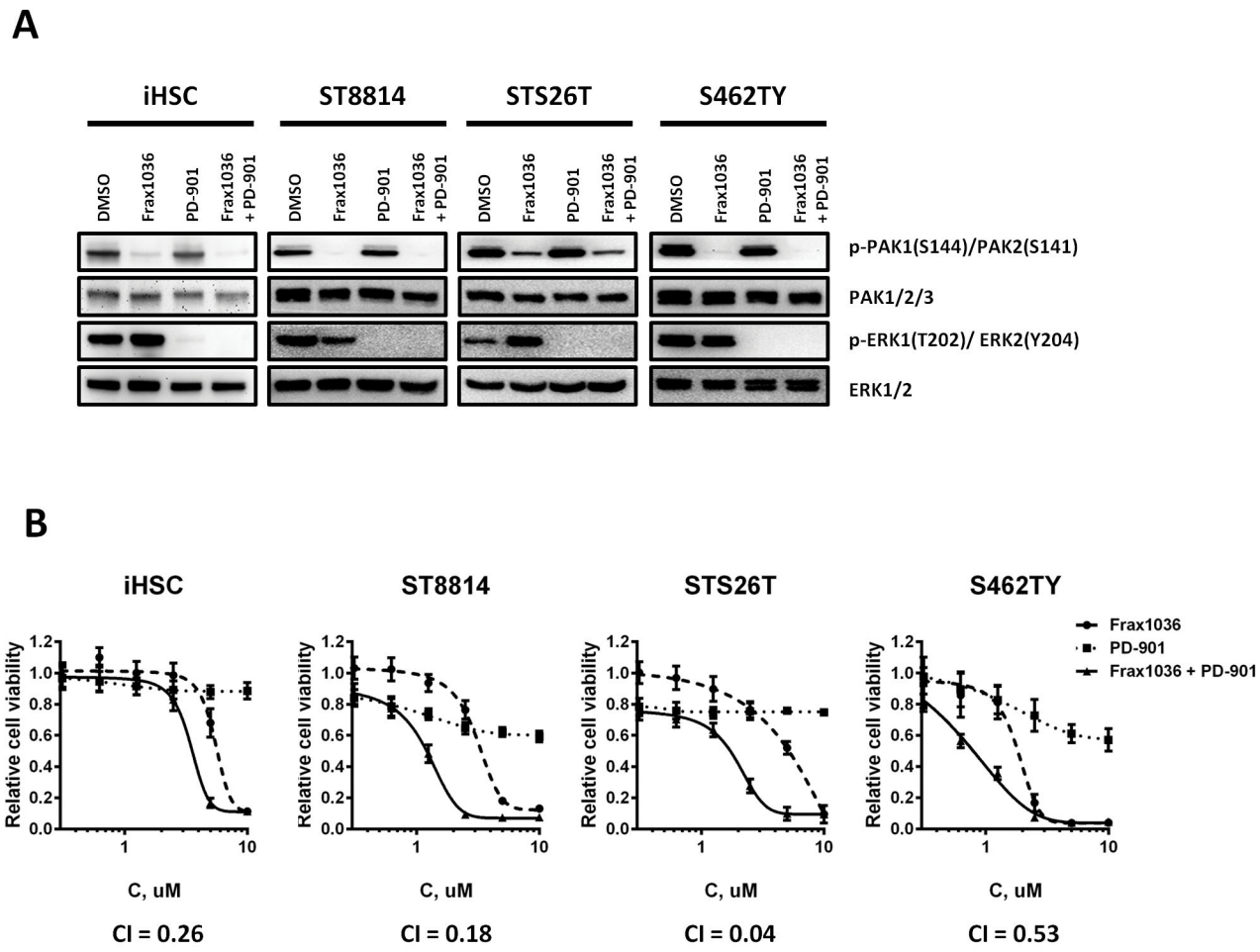

Figure 4. Frax1036 and PD-901 synergistically affect MPNST cell viability

A. Immunoblot analysis of PAK1/2/3 and ERK1/2 total protein and phospho-protein levels in iHSC, ST8814, STS26T and S462TY cells exposed to DMSO, Frax1036, PD-901, or a combination of Frax1036 and PD-901. **B**. Dose-response curves of iHSC and MPNST cells exposed to Frax1036, PD-901 or a combination of both compounds, combination indices (CI) for Frax1036 and PD-901 treatment.

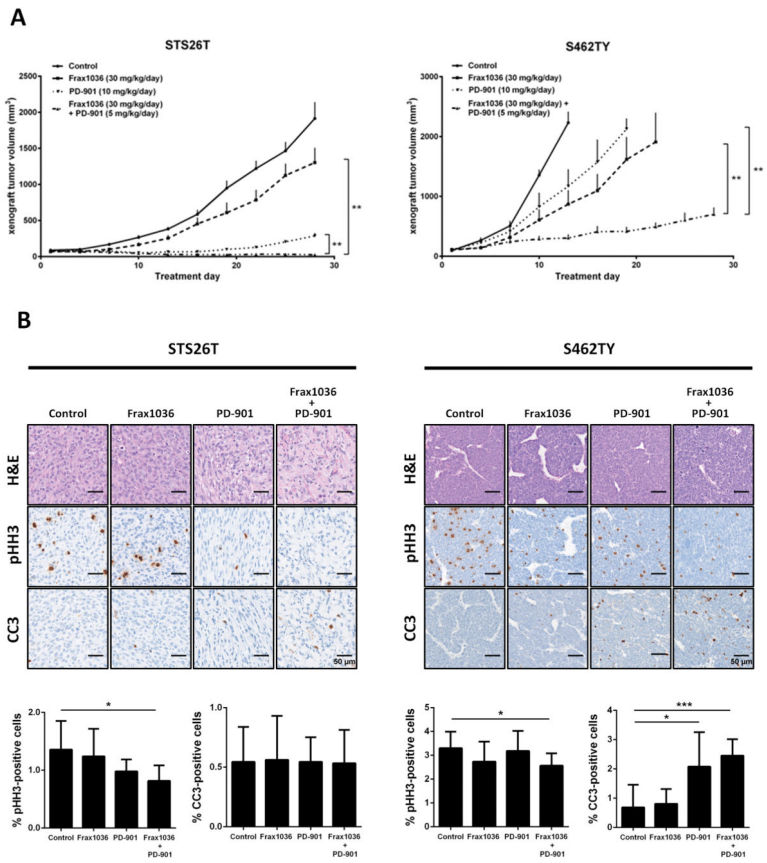

Figure 5. Frax1036 and PD-901 combination inhibits MPNST local tumor growth

Nu/nu immunodeficient mice bearing STS26T or S462TY subcutaneous xenograft tumors (~100 mm^3) were allocated into four groups (n=6) and exposed to vehicle only, Frax1036, PD-901 or combination of Frax1036 and PD-901 for a period of four weeks. **A**. Volumetric changes of STS26T and S462TY xenograft tumors in control and experimental groups. **B**. IHC analysis of phospho-histone H3 (pHH3) and cleaved caspase 3 (CC3) in all groups of STS26T and S462TY tumors at study termination. Error bars represent standard error of the mean (*= p<0.05, **= p<0.01).

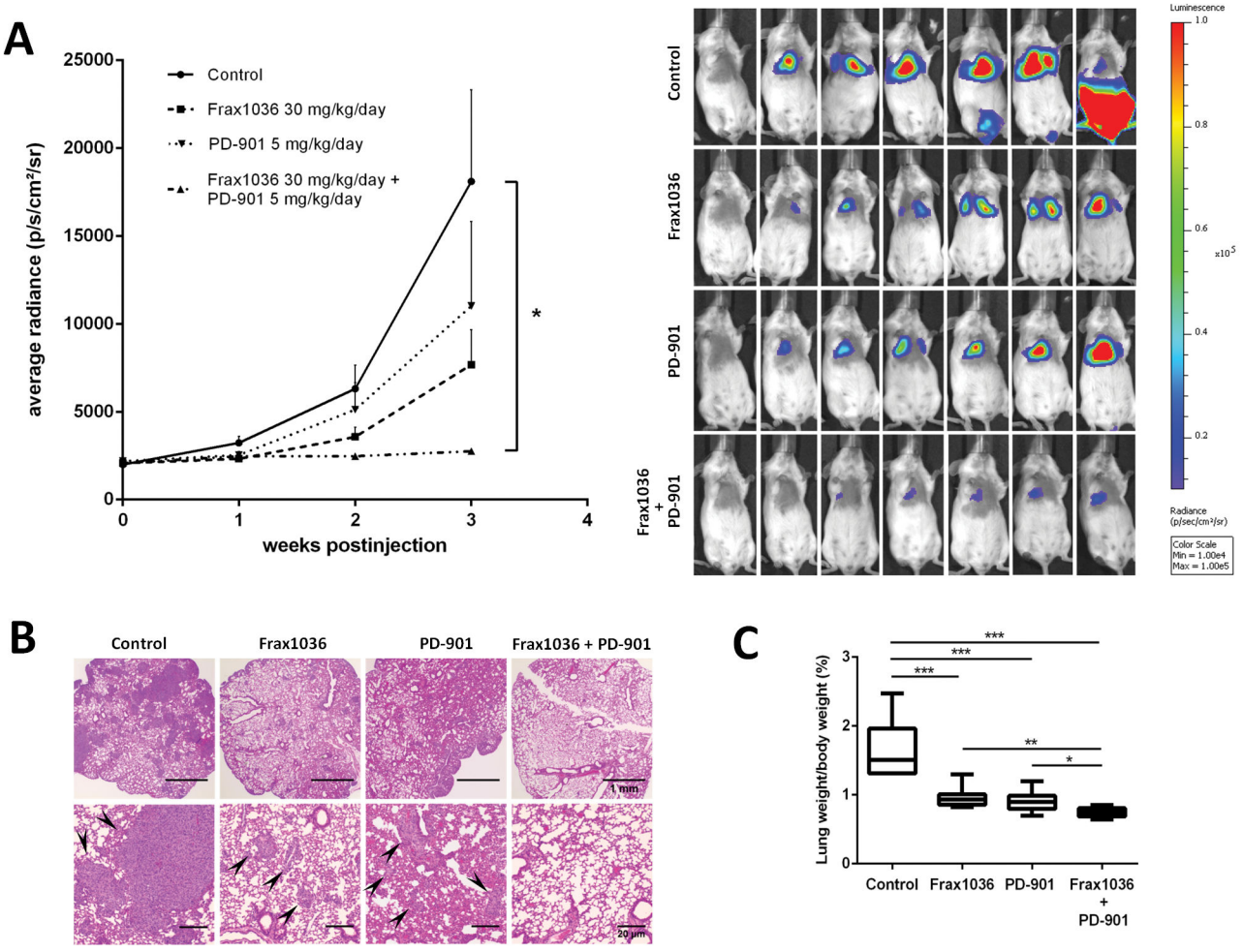

Figure 6. Frax1036 and PD-901 combination inhibits formation and growth of experimental MPNST metastasis

SCID immunodeficient mice tail-vein injected with STS26T-Luc were exposed to vehicle, Frax1036, PD-901 or a combination of Frax1036 and PD-901 in the course of three weeks. The kinetics of pulmonary tumor growth and spreading was monitored by BLI. **A.** Quantification of BLI signals in lung area of mice in control and experimental groups (n=7). Representative BLI images are shown on day 21 after grafting. **B**. Representative H&E sections of the lungs of mice from each group, showing lung tumor deposits (arrowed) in control, Frax1036 or PD-901 treated groups, but not in combinatorial treatment group. **C**. Quantification of relative lung weights in all groups at study termination. Error bars represent standard error of the mean (*= p<0.05, **= p<0.01, ***= p<0.005).